Imaging an atomic beam using fluorescence

Ming He (何 明), Jin Wang (王 谨), and Mingsheng Zhan (詹明生)

Laboratory of Magnetic Resonance and Atomic and Molecular Physics, Wuhan Institute of Physics and Mathematics, Chinese Academy of Sciences, Wuhan 430071

Received May 30, 2003

A fluorescence detection scheme is applied to image an atomic beam. Using two laser diodes as the sources of detection light and pumping light respectively, the fluorescence image of the atomic beam is then observed by a commercial CCD-camera, which is corresponding to the atomic state and velocity distribution. The detection scheme has a great utilization in the experiments of cold atoms and atomic optics.

OCIS codes: 020.0020, 110.2970, 140.3320.

The focusing of neutral atoms by using of various external fields has been the subject of intense interest recently. Atomic beam deflection experiments have substantially contributed to our understanding of the mechanical effects of external field on atoms. The first experiment to deflect atomic and molecular beams dated back to the pioneering work of Stern and Gerlach[1] in 1921, and then lots of experiments of deflection atomic beam using spontaneous resonance-radiation pressure were performed in 1980s[2,3]. For more than 40 years, focusing of atomic beams has been investigated and the formation of images of simple objects such as points or slits has been demonstrated[4,5]. Formerly, hot-wire ionization detectors are used to measure the intensity distribution of the atomic beam deflected by the external fields, such as magnetic and light fields. However, hot-wire ionization detectors are relatively slow and only capable of recording one-dimensional profiles of the atomic beam flux distribution. Recently, a new fluorescence detection scheme is applied to image the intensity distribution of an atomic beam in two dimensions and in real time[6,7].

To demonstrate the performance of our detection scheme we have carried out an atomic optics[8] experiment to realize an atomic guide[9,10] – a basic element of atomic optics. Our detection scheme is based on fluorescence imaging techniques, which have been successfully employed in different fields of research, e.g. ion trap[11], cold atoms[12–14]. We have adopted this imaging method to achieve high spatial and temporal resolution combined with detecting efficiency. The basic principle of the detection scheme is shown in Fig. 1.

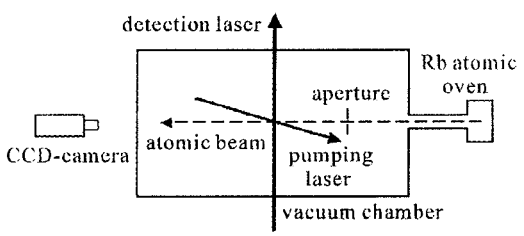

Fig. 1. Setup of the experiment. The frequencies of the lasers are tuned to various atomic resonance transitions, and the fluorescence is detected by a commercial CCD-camera. The detection laser beam passes orthogonally through the atomic beam and the pumping laser beam crosses the atomic beam at an angel of about 45°.

Employing two laser diodes (Toptica DL-100) and a commercial CCD-camera (Unican IIV-9961), we can obtain a fluorescence detection system that is versatile and independent of other experimental parameters.

In our experiment, the atomic source is an effusive oven with an opening of about 1mm in diameter. A rubidium atomic beam is collimated to 6.4 mrad full angle divergence by an aperture with a diameter of 2 mm, about 31 cm away from the oven. The CCD camera records the atomic density distribution about 15 cm downstream from the interaction zone.

To excite the Rb atoms we use two single mode laser diodes. One's frequency is electronically locked to the center of the Doppler-broadened $5S_{1/2}(F=3)$ to $5P_{3/2}(F=4)$ hyperfine transition near 780 nm of ^{85}Rb in a gas cell, and this laser beam is used as detection laser. To avoid the deflecting of the atomic beam owing to the interaction between the near resonant laser and the atomic beam, the power of the detection laser is set as weak as about 1mW. The other diode is locked to the center of the transition of $5S_{1/2}(F=2)$ to $5P_{3/2}(F=3)$, and we employ it as the pumping laser, which crosses the atomic beam at an angel of about 45° and overlaps the imaging zone of the detection beam. In the experiment, the power of the pumping laser is about 2 mW. The fluorescence of the atom beam is detected through another window of the vacuum chamber, which orientation is perpendicular to the radiation direction of the detection laser.

The number of photons emitted by each Rb atom passing through the detection light beam is somewhat limited by optical pumping. Figure 2 shows the electronic hyperfine levels of the Rb D_2-transtion. The detection laser is resonant with the $5S_{1/2}(F=3)$ to $5P_{3/2}(F=4)$ transition. However, there is a small amount leakage to the $5S_{1/2}(F=2)$ state. To avoid this, the second laser is tuned to the $5S_{1/2}(F=2)$ to $5P_{3/2}(F=3)$ transition and quickly pumps any atoms that leak to the $F=2$ state back to $F=3$. Thus each atom is capable of emitting much more photons and hence resulting an image of increased brightness.

When the detection light frequency is tuned about 40 MHz (this value is chosen arbitrarily in the experiment) to the red of the $5S_{1/2}(F=3)$ to $5P_{3/2}(F=4)$ transition of ^{85}Rb, we can obtain a fluorescence imaging

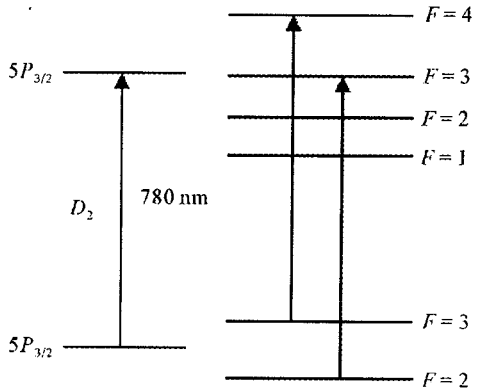

Fig. 2. Energy levels of the ^{85}Rb D_2 transition. Here the frequency of the detection laser is tuned near resonant with the $5S_{1/2}(F = 3)$ to $5P_{3/2}(F = 4)$ transition and the frequency of the pumping laser is tuned near resonant with $5S_{1/2}(F = 2)$ to $5P_{3/2}(F = 3)$ transition.

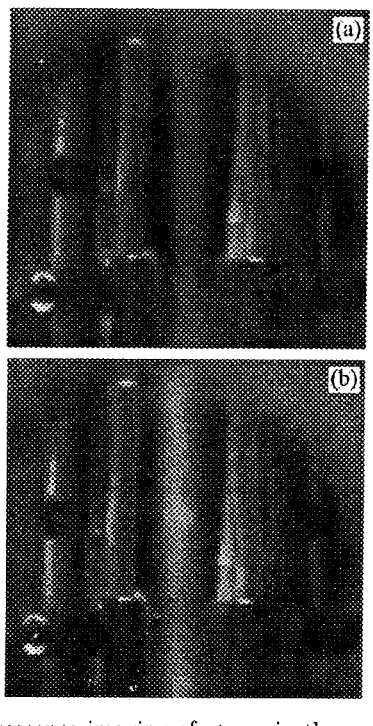

Fig. 3. Fluorescence imaging of atoms in the vacuum chamber. Here only the detection laser is employed. The frequency of the detection laser in subplot (a) is tuned to 40 MHz to the red of the $5S_{1/2}(F = 3)$ to $5P_{3/2}(F = 4)$ transition and the frequency in subplot (b) is tuned to 100 MHz to the blue of the $5S_{1/2}(F = 3)$ to $5P_{3/2}(F = 4)$ transition.

of atomic clouds in the vacuum chamber (Fig. 3(a)). There exists a bright stripe corresponding to the detected atoms and a homogeneous background of undetected atoms (those metal poles are the settings fixed in the experimental system). When the detection laser is tuned about 100 MHz to the blue of the $5S_{1/2}(F = 3)$ to $5P_{3/2}(F = 4)$ transition, we find that a brighter dot appears in the detection zone, whose density distribution corresponds to the shape of the atomic beam cross section (Fig. 3(b)).

Figure 4 gives the absorption Doppler profile of ^{85}Rb, which is obtained from the gas cell. Here two small peaks Co(3, 2−4) and Co(3, 3−4) are shown, which are the crossover peaks[15] of the hyperfine transition of $5S_{1/2}(F = 3)$ to $5P_{3/2}(F = 4)$ and can be employed as reference marks of the frequency of the detection laser. The absorption peak P(3, 4) [about 100 MHz away from the peak Co(3, 2−4)] is set as the zero point, and the arrows (a) and (b) mark the frequencies of the detection laser mentioned in previous paragraph. It can be observed that the arrow (b) almost located at the middle of the Doppler profile. In our experiment, the temperature of the Rb atomic Oven is set at about 200°C, corresponding that the most probability velocity of the thermal Rb atoms is about 300 m/s. From Fig. 4, we can estimate the velocity distribution of the detected atomic beam in Fig. 3(b) is just around the most probability velocity.

Up to now, we use only the detection laser diode to imaging the atomic beam. Then we employ an additional pumping laser diode to intensify the brightness of the image of the atomic beam in the plane of detection. Firstly, as same as previous step, we tune the detection light frequency 40 MHz to the red of the $5S_{1/2}(F = 3)$ to $5P_{3/2}(F = 4)$ transition and the pumping light frequency resonant with the $5S_{1/2}(F = 2)$ to $5P_{3/2}(F = 3)$ transition of ^{85}Rb. And then we observe that the atomic density distribution in the plane of detection consists of two stripes with uniform brightness. In the region of the intersection of two laser beams, the fluorescence is just a little brighter (Fig. 5(a)). Secondly, we tune the detection light frequency about 100 MHz to the blue of the $5S_{1/2}(F = 3)$ to $5P_{3/2}(F = 4)$ transition and the pumping light frequency still resonant with the $5S_{1/2}(F = 2)$ to $5P_{3/2}(F = 3)$ transition of ^{85}Rb. Similarly, a brighter dot is present in the intersection of two lasers (Fig. 5(b)). Compared with that in previous figure, here the image of the atomic beam is brighter and more distinguishable. Besides of this, due to the pumping laser crossing the atomic beam with an angel, the pumping laser only optically pumps atoms of one velocity class. So the fluorescence imaging is somewhat under the influence of the varying of the pumping laser frequency.

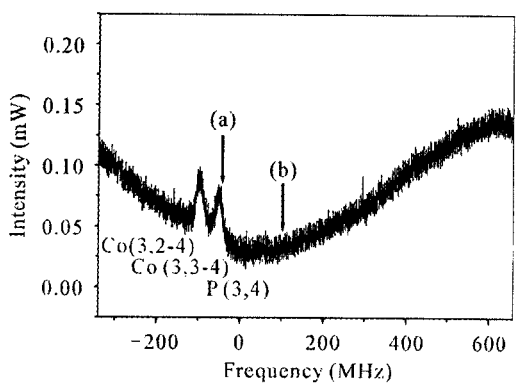

Fig. 4. Absorption Doppler profile of ^{85}Rb. Here two crossover peaks Co(3, 2−4) and Co(3, 3−4) are shown and the peak P(3, 4) is set as the reference zero of the laser frequency. The arrows (a) and (b) mark the frequenceis of the detection laser that tuned to −40 MHz and 100 MHz respectively.

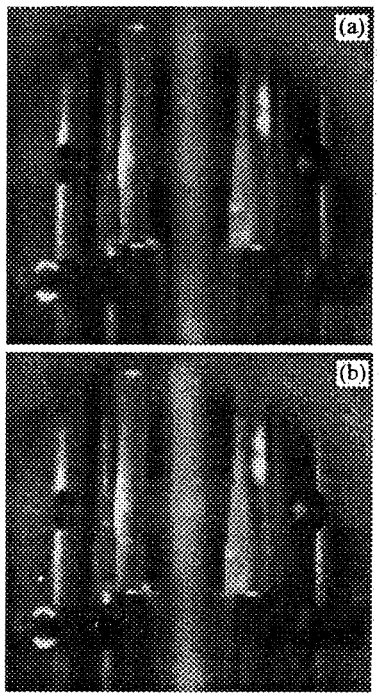

Fig. 5. Fluorescence imaging of atoms in the vacuum chamber. Here an additional pumping laser is used. The frequency of the pumping laser is tuned to resonant with the $5S_{1/2}(F = 2)$ to $5P_{3/2}(F = 3)$ transition of ^{85}Rb, and the frequencies of the detection laser in the subplots (a) and (b) are similar to those in Fig. 3.

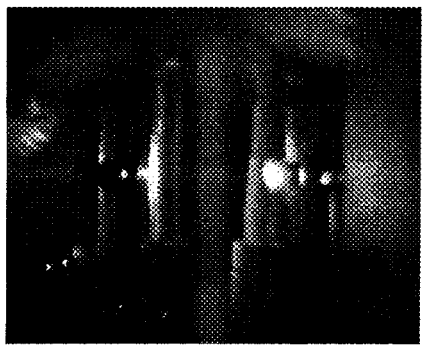

Fig. 6. Fluorescence imaging of longitudinal laser-slowed atomic beam by using the light chirp technique. Here the frequency of the detection laser is tuned about 200 MHz to the blue of the center of the Doppler profile, corresponding to the end frequency of the cooling chirp.

Because the fluorescence imaging is sensitive to the velocity distribution of the atomic beam, this detection scheme can be used to observe a slowed atomic beam. In our further experiment, a rubidium atomic beam is laser-slowed by the light chirp technique[16,17]. Applying counter-propagating radiation from a diode laser, the atomic beam absorbs photos from the counter-propagating laser beam and is slowed. The injection current of the cooling diode laser is coupled with a cooling chirp ramp whose frequency is tuned resonant with the $5S_{1/2}(F = 3)$ to $5P_{3/2}(F = 4)$ transition of ^{85}Rb. To avoid the leakage to the $F = 2$ ground state, a pumping laser is employed, whose frequency is tuned resonant with the $5S_{1/2}(F = 2)$ to $5P_{3/2}(F = 3)$ transition of ^{85}Rb. The cooling laser and pumping laser are superimposed and focused to overlap the rubidium atomic beam. The cooling chirp starts at a frequency to the left (low-frequency side) of the Doppler profile. The end frequency of the cooling chirp is about 200 MHz to the blue of the center of the Doppler profile. When the frequency of the detection laser is tuned as about the same as the end frequency of the cooling chirp, we can obtain a fluorescence imaging of the slowed atomic beam (Fig. 6).

In conclusion, we have test a detection scheme, which allows us to detect atomic beam through observing the fluorescence imaging. To do this, we employ a detection system that consists of two parts: two laser diodes tuned to various atomic transition frequencies and a commercial CCD-camera. Specially, the detection scheme brings us a great convenience to detect atoms of one longitudinal velocity class. It seems to be an effective and versatile tool to image an atomic beam and has a wide range of application in the experiments of cold atoms and atomic optics.

M. He's e-mail address is minghehu@wipm.ac.cn.

References

1. O. Stern, Z. Phys. **7,** 249 (1921); O. Stern and W. Gerlach, Z. Phys. **8,** 110 (1921).
2. Y. Z. Wang, R. F. Zhou, Z. R. Zhou, W. Q. Cai, G. Q. Ni, S. Y. Zhou, C. S. Wang, and W. J. Zhen, Science in China A **5,** 467 (1984).
3. J. E. Biorkholm, R. R. Freeman, and D. B. Pearson, Phys. Rev. A **23,** 491 (1981).
4. V. I. Balykin, V. S. Letokhov, Y. B. Ovchinnikov, and A. I. Sidorov, J. Mod. Opt. **35,** 17 (1988).
5. O. Carnal, M. Sigel, T. Sleator, H. Takuma, and J. Mlynek, Phys. Rev. Lett. **67,** 3231 (1991).
6. T. Esslinger, A. Hemmerich, and T. W. Hänsch, Opt. Commun. **93,** 49 (1992).
7. C. C. Bradley, J. J. McClelland, W. R. Anderson, and R. J. Celotta, Phys. Rev. A **61,** 053407 (2000).
8. C. S. Adams, M. Sigel, and J. Mlynek, Phys. Rep. **240,** 143 (1994).
9. J. Denschlag, D. Cassettari, and J. Schmiedmayer, Phys. Rev. Lett. **82,** 2014 (1999).
10. M. Key, I. G. Hughes, W. Rooijakkers, B. E. Sauer, and E. A. Hinds, Phys. Rev. Lett. **84,** 1371 (2000).
11. R. Blümel, C. Kappler, W. Quint, and H. Walther, Phys. Rev. A **40,** 808 (1989).
12. M. H. Anderson, J. R. Ensher, M. R. Matthews, C. E. Wieman, and E. A. Cornell, Science **269,** 198 (1995).
13. C. C. Bradley, C. A. Sackett, J. J. Tollett, and R. G. Hulet, Phys. Rev. Lett. **75,** 1687 (1995).
14. K. B. Davis, M. O. Mewes, M. R. Andrews, N. J. van Druten, D. S. Durfee, D. M. Kurn, and W. Ketterle, Phys. Rev. Lett. **75,** 3969 (1995).
15. K. B. MacAdam, A. Steinbach, and C. Wieman, Am. J. Phys. **60,** 1098 (1992).
16. R. N. Watts and C. E. Wieman, Opt. Lett. **11,** 291 (1986).
17. W. Ertmer, R. Blatt, J. L. Hall, and M. Zhu, Phy. Rev. Lett. **54,** 996 (1985).